



UNIVERSITÀ
DEGLI STUDI
FIRENZE

FLORE

Repository istituzionale dell'Università degli Studi di Firenze

3d printing of cardiac structures from medical images: an overview of methods and interactive tools

Questa è la Versione finale referata (Post print/Accepted manuscript) della seguente pubblicazione:

Original Citation:

3d printing of cardiac structures from medical images: an overview of methods and interactive tools /
Uccheddu, Francesca; Carfagni, Monica; Governi, Lapo; Furferi, Rocco; Volpe, Yary; Nocerino, Erica. - In:
INTERNATIONAL JOURNAL ON INTERACTIVE DESIGN AND MANUFACTURING. - ISSN 1955-2513. -
ELETTRONICO. - 12:(2018), pp. 597-609. [10.1007/s12008-017-0415-y]

Availability:

This version is available at: 2158/1087232 since: 2021-03-30T12:42:14Z

Published version:

DOI: 10.1007/s12008-017-0415-y

Terms of use:

Open Access

La pubblicazione è resa disponibile sotto le norme e i termini della licenza di deposito, secondo quanto
stabilito dalla Policy per l'accesso aperto dell'Università degli Studi di Firenze
(<https://www.sba.unifi.it/upload/policy-oa-2016-1.pdf>)

Publisher copyright claim:

(Article begins on next page)

Dear Author,

Here are the proofs of your article.

- You can submit your corrections **online**, via **e-mail** or by **fax**.
- For **online** submission please insert your corrections in the online correction form. Always indicate the line number to which the correction refers.
- You can also insert your corrections in the proof PDF and **email** the annotated PDF.
- For fax submission, please ensure that your corrections are clearly legible. Use a fine black pen and write the correction in the margin, not too close to the edge of the page.
- Remember to note the **journal title**, **article number**, and **your name** when sending your response via e-mail or fax.
- **Check** the metadata sheet to make sure that the header information, especially author names and the corresponding affiliations are correctly shown.
- **Check** the questions that may have arisen during copy editing and insert your answers/ corrections.
- **Check** that the text is complete and that all figures, tables and their legends are included. Also check the accuracy of special characters, equations, and electronic supplementary material if applicable. If necessary refer to the *Edited manuscript*.
- The publication of inaccurate data such as dosages and units can have serious consequences. Please take particular care that all such details are correct.
- Please **do not** make changes that involve only matters of style. We have generally introduced forms that follow the journal's style. Substantial changes in content, e.g., new results, corrected values, title and authorship are not allowed without the approval of the responsible editor. In such a case, please contact the Editorial Office and return his/her consent together with the proof.
- If we do not receive your corrections **within 48 hours**, we will send you a reminder.
- Your article will be published **Online First** approximately one week after receipt of your corrected proofs. This is the **official first publication** citable with the DOI. **Further changes are, therefore, not possible.**
- The **printed version** will follow in a forthcoming issue.

Please note

After online publication, subscribers (personal/institutional) to this journal will have access to the complete article via the DOI using the URL: [http://dx.doi.org/\[DOI\]](http://dx.doi.org/[DOI]).

If you would like to know when your article has been published online, take advantage of our free alert service. For registration and further information go to: <http://www.link.springer.com>.

Due to the electronic nature of the procedure, the manuscript and the original figures will only be returned to you on special request. When you return your corrections, please inform us if you would like to have these documents returned.

Metadata of the article that will be visualized in OnlineFirst

Please note: Images will appear in color online but will be printed in black and white.

ArticleTitle 3D printing of cardiac structures from medical images: an overview of methods and interactive tools

Article Sub-Title

Article CopyRight Springer-Verlag France
(This will be the copyright line in the final PDF)

Journal Name International Journal on Interactive Design and Manufacturing (IJIDeM)

Corresponding Author

Family Name	Carfagni
Particle	
Given Name	Monica
Suffix	
Division	Department of Industrial Engineering
Organization	Università degli Studi di Firenze
Address	via di Santa Marta, 3, 50139, Florence, Italy
Phone	+39-055-2758731
Fax	
Email	monica.carfagni@unifi.it
URL	
ORCID	http://orcid.org/0000-0002-3393-7014

Author

Family Name	Uccheddu
Particle	
Given Name	Francesca
Suffix	
Division	Department of Industrial Engineering
Organization	Università degli Studi di Firenze
Address	via di Santa Marta, 3, 50139, Florence, Italy
Phone	
Fax	
Email	
URL	
ORCID	

Author

Family Name	Governi
Particle	
Given Name	Lapo
Suffix	
Division	Department of Industrial Engineering
Organization	Università degli Studi di Firenze
Address	via di Santa Marta, 3, 50139, Florence, Italy
Phone	
Fax	
Email	

	URL	
	ORCID	
Author	Family Name	Furferi
	Particle	
	Given Name	Rocco
	Suffix	
	Division	Department of Industrial Engineering
	Organization	Università degli Studi di Firenze
	Address	via di Santa Marta, 3, 50139, Florence, Italy
	Phone	
	Fax	
	Email	
	URL	
	ORCID	
Author	Family Name	Volpe
	Particle	
	Given Name	Yary
	Suffix	
	Division	Department of Industrial Engineering
	Organization	Università degli Studi di Firenze
	Address	via di Santa Marta, 3, 50139, Florence, Italy
	Phone	
	Fax	
	Email	
	URL	
	ORCID	
Author	Family Name	Nocerino
	Particle	
	Given Name	Erica
	Suffix	
	Division	
	Organization	Fondazione Bruno Kessler
	Address	Via Santa Croce, 77, 38122, Trento, Italy
	Phone	
	Fax	
	Email	
	URL	
	ORCID	
Schedule	Received	22 May 2017
	Revised	
	Accepted	24 May 2017
Abstract	The percutaneous interventions in the treatment of structural heart diseases represent nowadays a viable option for patients at high risk for surgery. However, unlike during the traditional open heart surgery, the heart structures to be corrected are not directly visualized by the physician during the interventions. The interpretation of the available medical images is often a demanding task and needs specific skills i.e. clinical experience and complex radiological and echocardiographic analysis. The new trend for	

cardiovascular diagnosis, surgical planning and intervention is, today, mutually connected with most recent developments in the field of 3D acquisition, interactive modelling and rapid prototyping techniques. This is particularly true when dealing with complex heart diseases since 3D-based techniques can really help in providing an accurate planning of the intervention and to support surgical intervention. To help the research community in confronting with this new trend in medical science, the present work provides an overview on most recent approaches and methodologies for creating physical prototypes of patient-specific cardiac structures, with particular reference to most critical phases such as: 3D image acquisition, interactive image segmentation and restoration, interactive 3D model reconstruction, physical prototyping through additive manufacturing. To this purpose, first, recent techniques for image enhancement to highlight anatomical structures of interest are presented together with the current state of the art of interactive image segmentation. Finally, most suitable techniques for prototyping the retrieved 3D model are investigated so as to derive a number of criteria for manufacturing prototypes useful for planning the medical intervention.

Keywords (separated by '-') Rapid prototyping - 3D modelling - Medical imagery - Heart - Cardiovascular diseases - Surgical planning

Footnote Information

3D printing of cardiac structures from medical images: an overview of methods and interactive tools

Francesca Ucheddu¹ · Monica Carfagni¹  · Lapo Governi¹ · Rocco Furferi¹ · Yary Volpe¹ · Erica Nocerino²

Received: 22 May 2017 / Accepted: 24 May 2017
© Springer-Verlag France 2017

Abstract The percutaneous interventions in the treatment of structural heart diseases represent nowadays a viable option for patients at high risk for surgery. However, unlike during the traditional open heart surgery, the heart structures to be corrected are not directly visualized by the physician during the interventions. The interpretation of the available medical images is often a demanding task and needs specific skills i.e. clinical experience and complex radiological and echocardiographic analysis. The new trend for cardiovascular diagnosis, surgical planning and intervention is, today, mutually connected with most recent developments in the field of 3D acquisition, interactive modelling and rapid prototyping techniques. This is particularly true when dealing with complex heart diseases since 3D-based techniques can really help in providing an accurate planning of the intervention and to support surgical intervention. To help the research community in confronting with this new trend in medical science, the present work provides an overview on most recent approaches and methodologies for creating physical prototypes of patient-specific cardiac structures, with particular reference to most critical phases such as: 3D image acquisition, interactive image segmentation and restoration, interactive 3D model reconstruction, physical prototyping through additive manufacturing. To this purpose, first, recent techniques for image enhancement to highlight anatomical structures of interest are presented together with the current state of the art of interactive image segmentation. Finally, most suitable techniques for prototyping the retrieved 3D

model are investigated so as to derive a number of criteria for manufacturing prototypes useful for planning the medical intervention.

Keywords Rapid prototyping · 3D modelling · Medical imagery · Heart · Cardiovascular diseases · Surgical planning

1 Introduction

Thanks to the outstanding advances in both paediatric cardiology and cardiac surgery, the number of children affected by congenital heart disease (CHD) surviving into adulthood continues to increase [1]. Therefore, adults with CHD represents an ever-growing population, of around 3 million patients in Europe [2], with continues to increase by 5% per year. It is therefore not surprising that the care, and management, of adult patients with congenital or acquired structural heart disease represents one of the most relevant areas of research in cardiology, documenting a grow of studies related to this vital area [3–5].

Given the widely-ranged complexity of possible structural heart defects, imaging is paramount in their treatments. Although two-dimensional (2D) imaging modalities such as echocardiography, computed tomography (CT), and magnetic resonance imaging (MRI) are undeniably valuable in the evaluation of adult patients with structural heart disease, these methods are still constrained by their overall lack of realism and inability to be “physically manipulated”; thereby, such techniques remain limited in their ability to effectively represent the complex three-dimensional (3D) shape of the heart and its peripheral structures. Quite the opposite, 3D medical data representation, obtained from medical imagery, has the potential of providing information concerning heart structure, giving at the same time the opportunity

✉ Monica Carfagni
monica.carfagni@unifi.it

¹ Department of Industrial Engineering, Università degli Studi di Firenze, via di Santa Marta, 3, 50139 Florence, Italy

² Fondazione Bruno Kessler, Via Santa Croce, 77, 38122 Trento, Italy

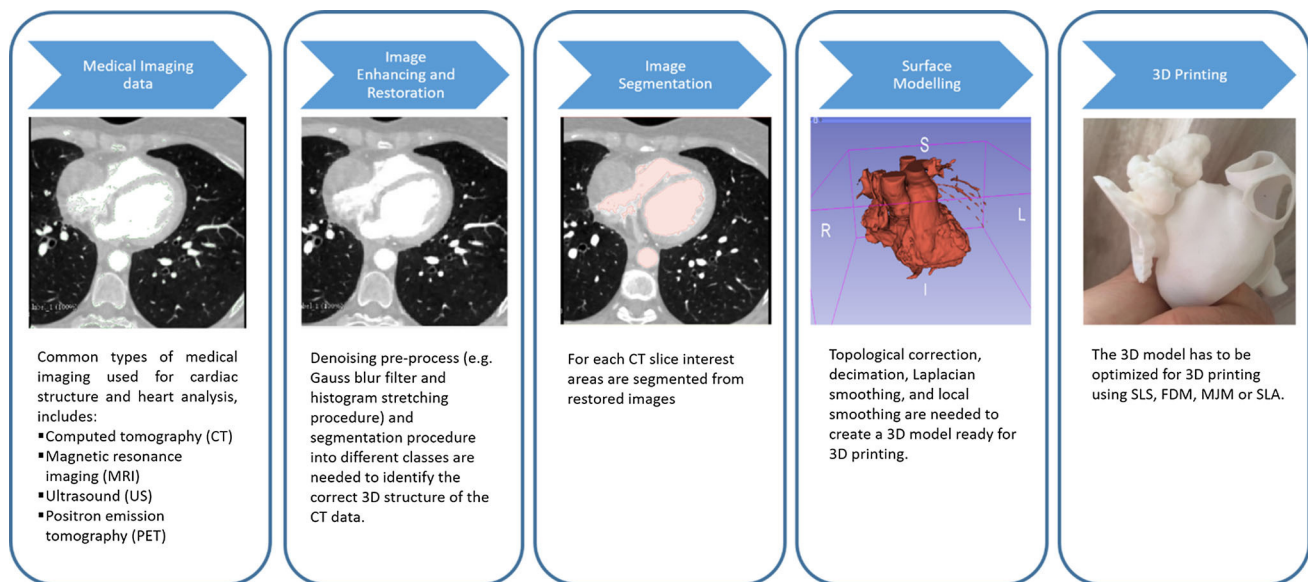


Fig. 1 Patient-specific 3D modelling and printing workflow

of further investigations when combined with additive manufacturing methods and technology. Recently, a number of most advanced hospitals [6–8] introduced in their praxis the use of physical 3D models of the patient cardiac structure to be used for surgical planning or for training.

These few cutting-edge experiences suggested that the progress of 3D printing technology sector can provide a number of advanced tools helping the medical staff to confront with care and management congenital or acquired structural heart diseases. In fact, the possibility of creating a patient-specific tangible 3D fabricated model provides medical staff with information that goes beyond a simple 3D-shaded visualization on a flat screen. The “zero lead time” between design and final production of accurate models together with the possibility of creating specific models resembling the actual structure of the patient heart accelerate the recent medical trend towards “personalized” or “patient-specific” treatment.

According to recent literature [9, 10], the most effective way for creating 3D models starting from 2D medical imaging is based on a virtuous process cycle that usually starts from 2D and 3D medical image acquisition and ends with 3D printing of a model of the patient heart (see Fig. 1).

In detail, such a process starts from medical imagery with particular reference to (but not exclusively) CT, multi-slice CT (MCT) and MRI. All these methods basically [11–14] provide 3D information in the form of cross-sectional “slices” of the entire body or parts of interest. Such slices consist of digital pictures stacked through the measurement volume, where each pixel represents the spatial position of the imaged element and its colour (usually in grey values) the reaction of the tissue to radiation or magnetic field (in

case of CT and MRI respectively). Acquired images are then processed, usually by using semi-automatic and interactive methods, in order to segment regions of interest, e.g. heart chambers, valves, aorta and coronary vessels. These segmented areas are, then, converted into 3D models, using tools like volume rendering or surface reconstruction procedures. This process is very useful in clinical practice, since it allows for interactive and easy visualization of different tissues and anatomical structures. Surface reconstruction techniques provide 3D polygonal mesh model of the external surface of the part. The obtained 3D surface models are useful for performing dimensional verification (volume computation, thickness and centreline of blood vessels calculation, etc.), structural analysis (e.g. by using finite elements FE) and computational fluid dynamics (CFD) studies. Moreover, the availability of topologically correct and optimized surface models allows the manufacturing of a prototype of cardiac structure, using for instance additive manufacturing techniques.

Due to the increasing number of methods to comply with the above mentioned process, and since such a virtuous process has been only recently introduced in clinical practice, the main aim of the present work is to provide an overview of methodologies dealing with patient-specific 3D modelling of cardiac structures. First, main imaging systems medical imagery for acquiring 2D and 3D data inferred to heart structure are introduced (Sect. 2). Then, the most adopted algorithms for image enhancement and restoration are explored (Sect. 3) and an overview of interactive segmentation and classification algorithms is described (Sect. 4). Section 5 is devoted to briefly overview most promising techniques for 3D heart model reconstruction process. Finally, in

124 Sect. 6, some considerations regarding 3D printing of heart
125 structure are draft.

126 2 Medical imaging

127 Since the discovery of X-rays by Wilhelm Conrad Rontgen
128 in 1895, medical images have become a major component of
129 diagnostics, treatment planning and procedures, and follow-
130 up studies. Moreover, medical images are increasingly used
131 for education, documentation, and research since they pro-
132 vide description of morphology as well as physical and
133 biological functions in 1D, 2D, 3D, and even 4D image data
134 (e.g., cardiac MRI, where up to eight volumes are acquired
135 during a single heart cycle) [15]. Today, a large variety of
136 imaging modalities have been established; these are mainly
137 based on transmission, reflection or refraction of light, radi-
138 ation, temperature, sound, or spin. Most imaging techniques
139 are non-invasive, allowing to seek for internal structures of
140 the patient's body hidden by skin and bones. The output of
141 the imaging acquisition process and input of the rapid proto-
142 typing following appropriate processing is a DICOM image
143 (Digital Imaging and Communications in Medicine), which
144 is the, traditional, virtual outcome of all medical professions
145 utilizing images [16].

146 Over the years, a number of different medical imaging
147 modalities has been developed, using different technologies
148 and creating several kinds of images. Common types of med-
149 ical imaging include: (i) X-ray (radiography, CT, etc.), (ii)
150 MRI, (iii) ultrasound, (iv) nuclear medicine (e.g., positron
151 emission tomography—PET).

152 2.1 Magnetic resonance imaging (MRI)

153 MRI is an imaging technique based on detecting different
154 tissue characteristics by varying the number and sequence
155 of pulsed radio frequency fields, taking advantage of the
156 magnetic relaxation properties of different tissues [17]. MR
157 imaging has the crucial advantage of not emitting X-ray radi-
158 ations. Instead, the MR scanner provides a strong magnetic
159 field, which causes protons to align parallel or anti-parallel
160 to it. MR measures the density of a specific nucleus, nor-
161 mally hydrogen, which is magnetic and largely present in
162 the human body, including heart [18], except for bone struc-
163 tures. The speed at which protons lose their magnetic energy
164 varies in different tissues allowing detailed representation of
165 the region of interest. This measurement system is volumet-
166 ric, producing isometric 3D images (i.e. the same resolution
167 in all directions).

168 2.2 Computerized tomography (CT)

169 As widely known, CT combines many X-ray images, taken
170 from different angles, to produce cross-sectional (i.e. tomo-

171 graphic) images of patient areas. Especially in the recent
172 advances, CT can provide detailed anatomical information of
173 chambers, vessels, coronary arteries, and coronary calcium
174 scoring. In particular, two imaging techniques are typically
175 carried out in cardiac tomography: (1) coronary calcium scor-
176 ing with non-contrast CT and (2) non-invasive imaging of
177 coronary arteries with contrast-enhanced CT. Usually, *non-*
178 *contrast CT* imaging exploits the natural density of tissues.
179 As a result, various densities using different attenuation val-
180 ues such as air, calcium, fat, and soft tissues can be easily
181 distinguished. Non-contrast CT imaging is a low-radiation
182 exposure method within a single breath hold, determining
183 the presence of coronary artery calcium.

184 In comparison, *contrast-enhanced CT* (see Fig. 2) is used
185 for imaging of coronary arteries with contrast material such
186 as a bolus or continuous infusion of a high concentration
187 of iodinated contrast material. Furthermore, coronary CT
188 angiography has been shown to be highly effective in detect-
189 ing coronary stenosis. Moreover, coronary CT angiography
190 can visualize not only the vessel lumen but also the vessel
191 wall, allowing non-invasive assessment of the presence and
192 the size of the non-calcified coronary plaque.

193 2.3 Ultrasound

194 In contrast to CT and MRI, ultrasound is a medical imaging
195 modality that is based on reflection of sound waves. Depend-
196 ing on the transducer, 1D to 4D data is obtained. In the 1D
197 case (signal), a longitudinal sound wave is traveling through
198 the tissue of the human body. At transitions between differ-
199 ent matter (e.g., muscle and fat), the sound wave is partly
200 reflected and transmitted (refracted if the surface is not hit
201 perpendicular).

202 Therefore, the echo runtime indicates the distance between
203 transducer and tissue border while the echo strength is
204 related to material properties. For cardiac usage, ultrasound
205 is applied by means of an echocardiogram able to provide infor-
206 mation on the four chambers of the heart, the heart valves and
207 the walls of the heart, the blood vessels entering and leaving
208 the heart and the pericardium. Echocardiography was, for a
209 long time, limited to a 2-D examination. As 3D ultrasound
210 is being more widely studied, new applications for imaging,
211 visualization and quantification of the heart are emerging. As
212 3D ultrasound images (see for instance Fig. 3) are typically
213 acquired in smaller sectors, to maintain adequate spatial and
214 temporal resolution, registration can be used to fuse multiple
215 3D sectors together; this extends the field of view, allow-
216 ing the quantification of larger structures while preserving
217 resolution [19].

218 2.4 PET

219 Positron emission tomography (PET) is a non-invasive med-
220 ical imaging modality that produces functional rather than

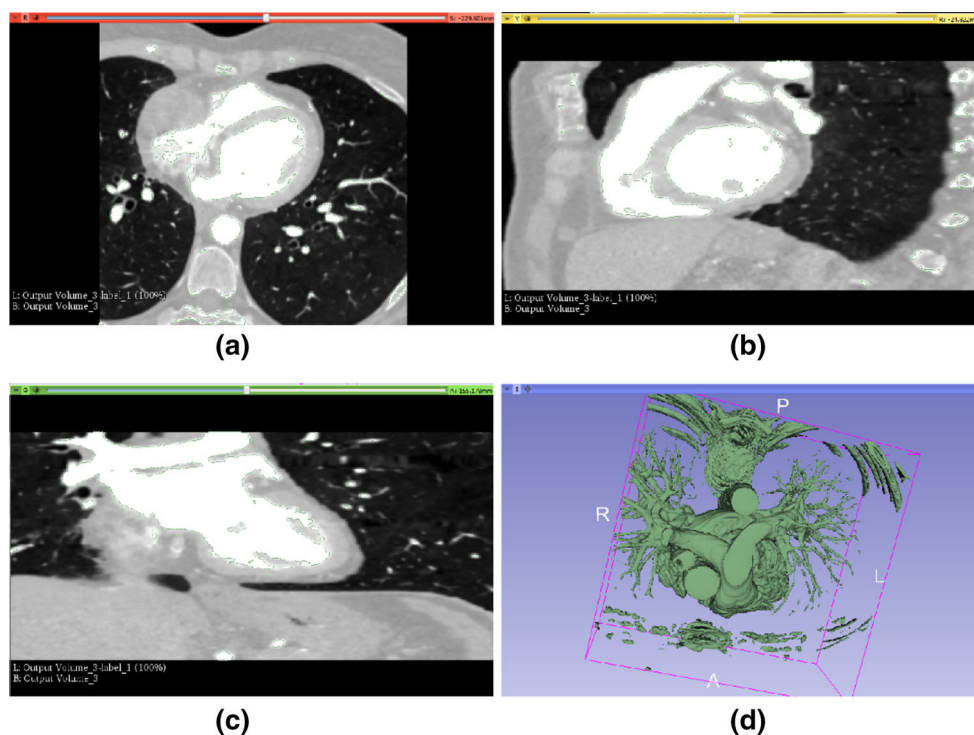


Fig. 2 CT scan with contrast in diastolic phase: **a** axial view; **b** sagittal view; **c** coronal view; **d** rough 3D reconstruction from originally acquired images (i.e. without post processing phases), demonstrating the necessity of enhancing and restoring the input image prior to proceed with 3D model reconstruction

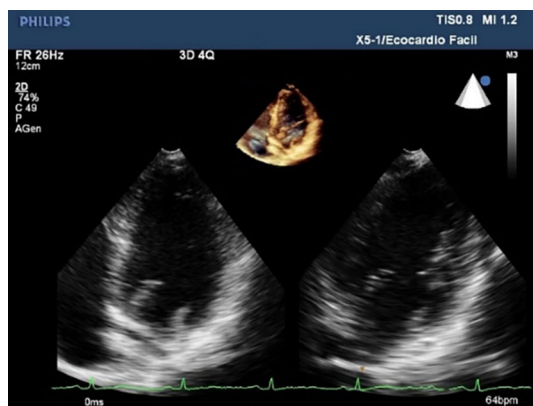


Fig. 3 Ultrasound image of a patient heart

2.5 Remarks

CT, PET, MRI provide, as said before, 3D information in the form of thin cross-sectional “slices” of the entire body or parts of interest, and are, therefore, called tomography imagery. The slices are provided in the form of digital pictures stacked through the measurement volume, where each pixel represents the spatial position of the imaged element and its colour (grey or RGB values) the reaction of the tissue to radiation (X-rays or gamma-rays) or magnetic field, in case of CT, PET and MRI respectively. Each of the above-mentioned imaging methods has its own advantages and disadvantages, both for potential patient’s health hazard (some of them require exposure to radiation) and information gathered and displayed. For example, CT and MRI are sensitive to different tissues properties, so that soft tissues are poorly visible in CT images, while they are distinctly evident in MRI.

3 Image restoration and enhancement

Digital medical imagery can be prone to degradation, due to several factors like patient motion or interferences, poor contrast, noise and blur. The artefacts are often intrinsically tied to the image acquisition method (e.g., X-rays show low contrast for soft tissues, ultrasound produces noisy images,

anatomical images, thereby providing greater insight to the patient’s condition. Functional imaging means that the body’s metabolism is being shown, as opposed to its structure. In a cardiac PET scan, the patient is administered with a drug that creates an effect in the body that is similar to exercise. Images of the myocardial blood flow are taken both before and after the induced stress and the images are compared to examine blood flow through the heart to determine if narrowing of the coronary arteries is restricting maximum blood flow [20]. PET can also identify dead tissue and injured tissue that’s still living and functioning.

and metallic implants cause imaging artefacts in MRI [21]). A huge number of methods for enhancing the quality and for restoring acquired data have been proposed in literature. To enhance the visual quality of medical images, the two main procedures are image restoration and image enhancement.

Image restoration algorithms act to denoise the images also by reducing the blur effect due to the data acquisition pipeline [22]. Denoising methods are based on the estimation and modelling of the blur and noise affecting the image. The main factors that influence the models include capturing sensors system, transmission media, image digitization, etc.

Enhancement belongs to the branch of digital image processing techniques that manipulate a digital image [23–25] to enhance the contrast, in order to extract, or accentuate, certain image features to improve the understanding of information content and obtain an image ready for automated image processing (e.g. for highlighting structures such as tissues and organs).

As mentioned above, restoration and enhancement methods for medical images depends on the imaging system. Therefore, an overview of most relevant methods is provided below.

3.1 Enhancing and restoration of MRI images

The main issue for cardiac images acquired using MRI is related to intensity non-uniformity, i.e. a smooth intensity variation across the image, resulting in biased intensities for the same tissue according to its location. Barely noticeable to a human observer, this distortion influences the subsequent steps of segmentation and classification. In fact, most of the automated, or interactive, quantitative methods for segmentation rely on the assumption that a given tissue has a similar voxel intensities throughout the data, so these methods are highly sensitive to variations on image intensities [26–28].

Numerous methods were developed to solve the intensity non uniformity problem; roughly these methods can be classified into three main groups:

- 1) Filtering methods: assumes that the non-uniformity is a low-frequency artefact that can be separated from the high-frequency signal of the imaged object by a low-pass filtering. Two main approaches can be followed to filter the original image: homomorphic filtering [29] and homomorphic unsharp masking (HUM) [30]. These methods are affected by other image features, such as edge effects, most present in high contrast images. Accordingly, some methods have been proposed to minimize these effects [26].
- 2) Surface fitting models. Since intensity non-uniformity is slowly varying, it is reasonable to approximate it by a parametric smooth function. As a consequence, the image correction can be addressed by dividing (voxel-by-voxel)

the original image by the computed surfaces. The different algorithms using surface fitting models vary in the way the fitting is performed; moreover, these methods are linked to image segmentation, which leads to frameworks that simultaneously correct the non-uniformity and perform the segmentation [31].

- 3) Statistical methods. The statistical methods assume that the intensity non-uniformity follows a statistical distribution. In fact, Edelstein et al. [32] showed that pure noise in magnitude images is governed by the Rayleigh distribution. As a consequence, it is possible to apply well-known look-up table correction schemes like the ones proposed in [33,34]. These methods are among the most used when dealing with cardiac MRI images.

3.2 Enhancing and restoration CT images

The low contrast of CT images due to the large dynamic range acquisition (usually 16 bit) often does not allows to properly discriminate acquired regions of interest, especially when dealing with cardiac structures. The most common method for enhancing the quality of the image, and at the same time to better discriminate possible presence of pathologies, is to perform a histogram equalization (HE) followed by smoothing filters as demonstrated, for instance, in Fig. 4 [35]. The main feature in HE is to find the mapping function generated from the global histogram of an image, to obtain a uniform distribution in the corresponding output image. Unfortunately, traditional HE technique may introduce undesired effects such as level saturation or over-enhancement. To solve this issue, a range of methods are proposed in literature. Most relevant methods are adaptive HE method [36] and Bi-histogram equalization [37]. Fuzzy Logic and other IA-based methods have been also explored to remove image artefacts [38].

3.3 Enhancing and restoration of ultrasound images

Ultrasound images have, in general, low signal to noise ratio (SNR) mainly due to pulsed signals that have short duration in time and therefore a broad spectrum in frequency domain [39]. Moreover, the coherent nature of the signals gives rise to speckle noise; finally, sound waves are highly distorted when traveling through the tissues. Consequently, the acquired images are speckled and present multiple defects such as, for instance, reflections represented by parallel bright lines or by the so called “comet tail”. Most errors are strongly avoidable by pre-processing techniques in ultrasound imaging. However, the acquired image is still to be enhanced. To this purpose a large number of methods have been proposed in literature, roughly classified in filtering methods and deconvolution methods. Since noise in ultrasound has been modelled as the combination of an additive error (e.g. elec-

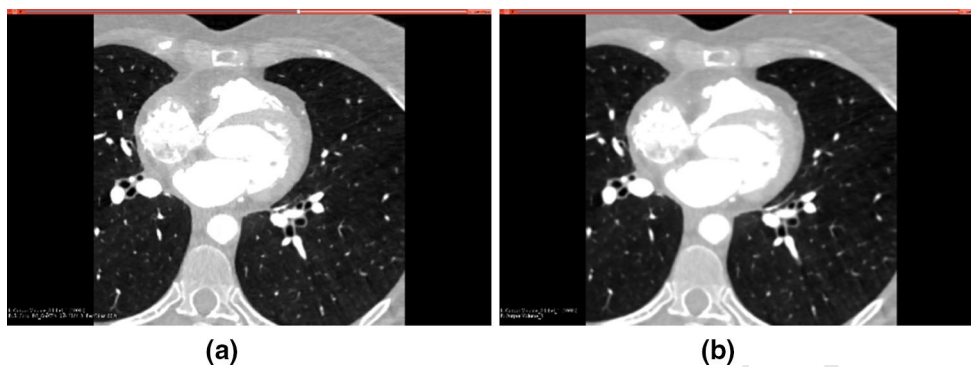


Fig. 4 **a** Original image; **b** restored image obtained by applying a histogram equalization followed by a Gaussian filter with a sigma value (SD) equal to 0.6 mm

tronic or thermal noise) with a multiplicative error (speckle), filtering algorithms are required to be adaptable to the noise properties across the image. Consequently, ultrasound filtering techniques include adaptive filters based on local statistics [40], anisotropic diffusion [41] and wavelets [42].

Differently from filtering approaches, deconvolution is a technique used to improve resolution in ultrasound images by counteracting the effect of the Point spread function (PSF) of the imaging device i.e. the response of the system to an ideal point target caused by diffraction spreading of the ultrasound signals [43]. If the PSF is known, its effects on the image can be eliminated by dividing the spectrum of the image by the spectrum of the PSF. In case the PSF is not known, it can be estimated based on the image itself [44] (this is called “blind deconvolution”).

3.4 Enhancing and restoration of PET images

PET image artefacts are primarily due to metallic implants, use of contrast media and respiratory motion. In particular, metallic implants (e.g. dental implants or metallic clips) are visualized by CT images as areas of high density [45]. Analogously, the presence of a contrast media can introduce errors in PET images similar to the ones produced by metallic implants. Both these errors, however, can be addressed directly by the medical staff by contouring the contrast regions and by excluding them from the image analysis [46].

Respiratory motion, instead, can induce an erroneous attenuation correction: because of respiratory motion the density of a particular organ could be attributed to an area whose density is different. This issue is far to be solved today since the best way to correct for respiratory motion would be to acquire gated images to discriminate different intervals of a breath cycle. Therefore, for examining PET images it is still crucial the help from medical staff and only a few approaches for interactive or automatic image enhancement are nowadays available [47].

4 Segmentation and classification

Segmentation is the process of dividing an image into a set of semantically meaningful, homogeneous, and non-overlapping regions with similar properties such as grey level, colour, texture, brightness, and contrast [48]. In medical imagery, the segmentation consists in identifying and subdividing different anatomical structures or regions of interest (ROI) in the images resulting in a partition of the image pixels in non-overlapping regions, belonging to the same tissue class.

Automatic segmentation of medical images is a valuable tool to perform a tedious task with the aim of making it faster and, ideally, more robust than manual procedures. However, it is a difficult task as medical images are complex in nature and often affect by intrinsic issues such as mixing up of tissue types, biased intensity, presence of artefacts, and closeness, in grey values for different tissues. As demonstrated in [49] a number of different approaches have been developed for automatic image segmentation that is still a current and active area of research.

Unfortunately, anatomical variability and intrinsic image issues limit the reliability of fully automatic approaches. Moreover, there is a substantial mistrust both from patients and doctors towards fully automatic algorithms. Accordingly, there has been a recent drive towards interactive segmentation [50]. Interactive approaches use a data-driven automatic algorithm to process a majority of the volume. As the automatic segmentation runs and displays the current state, a human user can influence the algorithm’s behaviour to more closely align with an expected result [51].

Interactive medical image segmentation employs software tools such as, for instance, Seg3D [52] and 3D-Slicer [53] for applying algorithms and, at the same time, visualizing the results (see Fig. 5). Another class of interactive methods makes use of active contour models, contour interpolation algorithms or their combination [54]. Graph Cuts [55] and CO3 approaches [56] are considered, further-

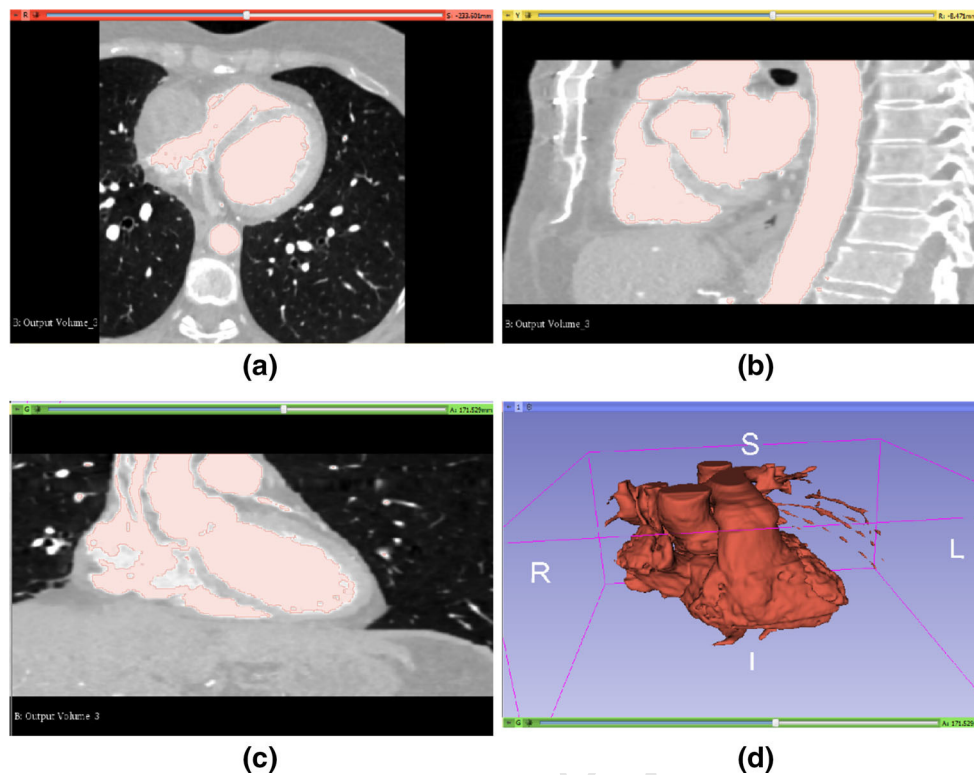


Fig. 5 Example of threshold-based interactive segmentation of a single slice for the aorta and left ventricle: **a** axial view; **b** sagittal view; **c** coronal view; **d** 3D reconstruction from restored images

426 more, golden standard techniques for performing interactive
427 segmentation.

428 Referring specifically to cardiac imaging, several segmen-
429 tation techniques have been further proposed [57]. Most of
430 the more recent studies focused on the segmentation of the
431 diastolic and systolic left ventricle, since the related volume
432 functional parameters are important predictors of heart dis-
433 eases [58].

434 Schneider et al. [59] proposed a method to segment the
435 Mitral annulus using graph-cuts. Zheng et al. [60] presented
436 a segmentation method based on the marginal space learning
437 by searching for the optimal smooth surface. Jolly [61] pro-
438 posed a method for extracting the myocardium in 4-D cardiac
439 MR and CT images using the graph-cuts as well as EM-based
440 segmentation. Model-based techniques were also adopted for
441 cardiac MRI or CT image segmentation using active shape
442 models with PCA [62], atlas-based segmentation [63,64],
443 methods for region growing [65,66], thresholding [67,68]
444 and machine learning approach using decision forests [69]
445 were also used.

446 5 3D heart model reconstruction for rapid 447 prototyping

448 As shown in [70], the generation of a 3D cardiac geometry
449 represented by a 3D surface mesh can be considered the very

450 first step of the construction process of a 3D cardiac model. It
451 has to be considered that the reconstructed geometry includes
452 one or several cardiac chambers (LV, bi-ventricular, atrial or
453 whole-heart models) and also other details such as the great
454 cardiac vessels including “outflow and/or inflow tracts [71–
455 73], the fibrous annulus of atrioventricular valves [74,75],
456 part of the coronary tree, or some endocardial details such
457 as papillary muscles and trabeculae carneae for ventricles
458 or crista terminalis, pectinate muscles and fossa ovalis for
459 atria [76–78]”. Moreover, it is important to highlight that
460 the anatomical accuracy required by a 3D cardiac model
461 depend on its final application. For instance, in [79] it was
462 concluded that structurally simplified models (without endo-
463 cardial details or vessels) are well suited for a large range of
464 3D cardiac modelling applications aimed at EP simulation.
465 Consequently, depending on the particular kind of applica-
466 tion of the 3D model, the main aim of 3D reconstruction is to
467 provide an accurate mesh after 3D image segmentation has
468 been carried out according to one of the methods described
469 in Sect. 4.

470 A surface model could be generated by using, for instance,
471 a marching cube method [80] or other 3D contour extraction
472 algorithms [81]. The resultant surface can be used as the start-
473 ing point for either generation of higher order representation,
474 such as non-uniform rational B-splines NURBS-based sur-
475 faces, or for meshing improvement using, for example, mesh

growing methods [82,83], Delaunay meshing techniques [84,85], descriptive geometry [86] or other voxel-based methods [87,88].

However, such an automatically retrieved 3D model is not suitable, as it stand, for 3D printing; this is due to a number of reasons such as, for instance, the presence of many separate mesh units and/or incomplete topological structure. Therefore, topological correction, decimation, Laplacian smoothing, and local smoothing [89,90] are usually needed to create a 3D model ready for 3D printing. In general, the accuracy of the 3D printing object depends on the combination of the accuracy of the medical image, which should be as thin as possible, the appropriate imaging process for 3D modelling, and the 3D printing accuracy of the system.

One major challenge faced in creating physical models lies in disconnection between the digital 3D surface models and the original 2D image. Currently available industry specific image-processing software applications remains limited in its ability to generate digital 3D models that are directly applicable to rapid prototyping. As a result, true integration of the raw 2D image data into the generated digital 3D surface models is lost. The post 3D processing (i.e., correction of errant points and elimination of various artefacts within the digital 3D surface model) therefore relies heavily on the expert clinical and anatomic knowledge of the graphic editor, especially because a wide array of structural heart anomalies that significantly deviate from conventional cardiovascular anatomy may be present. Once the surface model of the cardiac structure is interactively built, it is possible to manually add to the 3D model some important features such as, for instance, myocardial structure, cardiac conduction system and other patient-specific features (e.g. pathologies).

It is worth noting that the 3D reconstruction needed for the subsequent 3D printing process requires a continuous interaction between the users (engineers and medical staff) and the CAD software package used to perform the reconstruction. Without this interaction it is quite unfeasible to extract significant information from 3D images to create a complex 3D model of the anatomical part to be investigated. On a “higher” level, the proposed framework of Fig. 1 involves methods to virtually explore different solution spaces. In fact, once the images are acquired using one of the methods proposed in Sect. 2, different data can be reconstructed on the basis of which anatomy has to be modeled for medical purposes. Accordingly, users are required to virtually explore a number of possible CAD solutions by interacting with the acquired and pre-processed 3D data.

Another option to add myocardial structure is to estimate the fibre orientation associated to each element of the volumetric mesh of a model from pre-established patterns [91–94], most of them derived from Streeter’s findings [95]. The final result of the 3D reconstruction consists of a 3D

model representing the cardiac structure to be printed. As a consequence, despite several file formats exist, the model is almost universally stored in standard tessellation language (STL) format.

6 Additive technologies and 3D printing for cardiac structures

The most common additive technologies that can be used for prototyping cardiac structures are selective laser sintering, fused deposition modelling, multijet modelling/3D printing, and stereo-lithography. Selective laser sintering (3D Systems Inc., Rock Hill, SC) uses a high-power laser to fuse small particles of plastic, metal, or ceramic powders into a 3D object [96]. Selective laser sintering has the ability to utilize a variety of thermoplastic powders and has a high geometric accuracy but is generally higher in cost than other additive methods. In fused deposition modelling (e.g. from Stratasys Inc.), a plastic filament (typically acrylonitrile butadiene styrene polymer) is forced through a heated extrusion nozzle that melts the filament and deposits a layer of material that hardens immediately on extrusion. A separate water-soluble material is used for making temporary support structures while the manufacturing is in progress. The process is repeated layer by layer until the model is complete. Multijet modelling or 3D printing (Z Corporation, Burlington, Mass) essentially works like a normal ink-jet printer but in 3D space. In this process, layers of fine powder (either plaster or resins) are selectively bonded by printing a water-based adhesive from the ink-jet print head in the shape of each cross section as determined by the computer-aided design file. Each layer quickly hardens, and the process is repeated until the model is complete [97].

In stereolithography, models are built through layer-by-layer polymerization of a photosensitive resin. A computer-controlled laser generates an ultraviolet beam that draws on the surface of a pool of resin stimulating the instantaneous local polymerization of the liquid resin in the outlined pattern. A movable platform lowers the newly formed layer, thereby exposing a new layer of photosensitive resin, and the process is repeated until the model is complete.

Depending on their intended application (i.e. education, catheter navigation, device sizing and testing, and so on), physical models may be printed in multiple materials using a variety of 3D printing technologies, each with its own collection of benefits and shortcomings. For example, multijet modelling (see Fig. 5) technology can be used to generate full-colour models to highlight anomalous structures or specific regions of interest. Printing times are fast (approximately 6–7 h per model) and cost-effective (Fig. 6).

Although flexible models may be prototyped by multijet modelling technology, the properties of the material often

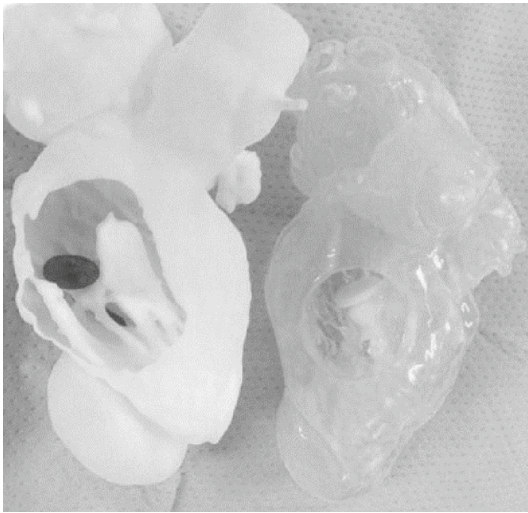


Fig. 6 Two examples of 3d printed models: on the *left* it is shown the model prototyped using multijet printer; on the *right*, the model realized using polyjet matrix technology is depicted

great vessels pathologies [100,101]. With reference to structural heart diseases, most relevant applications of 3D printing are related to the creation of patient-specific devices for closing the left atrial appendage [98] or for determining the ideal resection lines of the aneurysmectomy for patients affected by cardiac aneurysms [102]. Other studies report the use of 3D models for myectomies [103], atrial and ventricular septal defects [104]. Referring to aorta and vessel pathologies, a number of studies have been carried out to create 3D printed models of systemic vasculature; as stated in [9], in fact, “Rigid and flexible 3D-printed models can aid endovascular interventions by enabling the assessment of optimal stent dimensions and positioning in cases of transverse aortic arch hypoplasia”. Finally, 3D modelling of heart can be really helpful for education, training and decision-making [9,105]. Training on 3D printed models can be performed virtually anywhere, avoiding the cost and complexity of operating in the controlled environments required for animals and human cadavers.

7 Discussion and conclusions

With the development of inexpensive 3D printers, 3D printable multi-materials, and 3D medical imaging modalities, 3D printing medical applications for heart diseases among others, have come into the spotlight. Due to the availability of transparent, full-coloured, and flexible multi-materials, 3D printing objects can be more realistic, miming the properties of the real body; i.e., not only hard tissue alone but also hard and soft tissue together.

The study and experimentation conducted show that interactive approaches for image enhancement, segmentation, 3D modelling and printing have reached a promising point for medical applications. Moreover, the design framework introduced in Fig. 1 can be extended to other problems related to patient specific modelling since almost all medical interventions share techniques based on medical image acquisition and 3D reconstruction for diagnosis, education or intervention planning. It is therefore straightforward to add 3D printing methods to this traditional workflow, when the complexity of the anatomy to be treated requires physical models to be managed by medical staff. Some relevant examples can be found in hip and knees prosthesis design as well as in maxillofacial sector and in personalized hand-wrist-arm orthosis design. More in general, several different application areas can be interested in wide spreading 3D printing of cardiac structures. First, 3D printing can be really useful for aiding intervention planning, giving the medical staff the opportunity of handle a realistic and patient-specific model prior to proceed with the actual intervention. Secondly, the creation of 3D models is crucial for training; in fact, this can be performed virtually anywhere, avoiding the cost and complexity

fail to accurately mimic true tissue properties. PolyJet Matrix printing technology (see Fig. 5) offer the ability to print physical models in materials that more closely resemble the properties of native tissue, thus representing the new direction in rapid prototyping technology with its ability to print in different materials simultaneously. This unique technology will allow most physical models to be printed in durable materials (e.g., plastic), whereas specified segments (e.g., interatrial septum, septal defects, vascular structures, and so on) are printed in less durable, but more lifelike, materials (e.g. rubber polymers) for more realistic manipulation.

Given the broad spectrum of anatomic variations and pathologies, 3D printing could potentially be a game-changer in cardiology, particularly in challenging anatomies and rare pathologies, facilitating procedural planning, optimal sizing and simulation. The knowledge of the exact dimensions of the defect/communication/orifice that needs to be sealed and the relationship with adjacent structures is of paramount importance and often not readily available with conventional 2D imaging. 3D printing allows for direct visualization and simulation (trial and error) in order to identify the optimal device and angulation required to obtain the best possible result. The value of 3D printing in surgical pre-procedural planning lies primarily in the precise delineation of the underlying anatomy and is of paramount importance in complex congenital heart disease pre-procedural planning. Patient-specific implants and custom-made devices can be designed, produced, and tested, thus opening new horizons in personalized patient care and cardiovascular research.

A taxonomy of possible applications of 3D printing for cardiac structures can be found in [9] and mostly referred to paediatric and adult heart diseases [98,99] and to aorta and

of operating in the controlled environments required for animals and human cadavers. Finally, 3D modelling of heart can be really helpful for decision-making [9, 105] giving the medical staff the opportunity to test several different options specifically addressed to the patient own anatomy.

While the opportunity of using 3D printing for simulating medical surgery has been widely accepted in the medical field, for training purposes only a few studies are related to the impact on learning, all recalled in a review work [106] where authors demonstrate that despite there is no solid evidence that the use of 3D models is superior to traditional teaching, more studies are still needed to examine the short- and long-term impacts of 3D models on learning using valid and appropriate tools.

Development and optimization of the entire procedure, from image acquisition to 3D printing fabrication, are required for personalized treatment, even in emergency situations. In addition, to produce an effective 3D printing object, multidisciplinary knowledge of the entire 3D printing process chain is needed; namely, image acquisition using a protocol suitable for 3D modeling, post-processing of the medical images to generate a 3D reconstructed model, 3D printing manufacturing with an appropriate 3D printing technique, and post-processing of the 3D printing object to adapt it for medical use.

On the other hand, several major limitations, such as those associated with the technology and the time and cost of manufacturing 3D phantoms, remain to be overcome. In fact, during the virtual exploration of solutions for the 3D reconstruction the presence of artifacts could lead to erroneous medical interpretations. Therefore, the final model could provide wrong indications on geometry or, worst, on pathologies. To avoid these errors, that could strongly impact on the intervention planning or even on the actual medical surgery, the intervention of experts, interacting with CAD systems and/or with image processing-based algorithms is still needed to assess the accuracy of the final products and correct for errors that may occur during the automated phases of the procedure. Finally, an expanded heart team including physicians and engineers is needed to assess the correctness of the products and correct inaccuracies of automatic procedures, when translating the medical imaging into 3D printing. This opens, for the next future, the opportunity of creating new professionalism across medical science and engineering to confront with the incredible boost of methods and techniques related to 3D printing in biomedicine.

References

1. Moons, P., Engelfriet, P., Kaemmerer, H., Meijboom, F.J., Oechslin, E., Mulder, B.J.M.: Delivery of care for adult patients with

- congenital heart disease in Europe: results from the Euro Heart Survey. *Eur. Heart J.* **27**(11), 1324–1330 (2006)
2. Webb, C.L., Jenkins, K.J., Karpawich, P.P., Bolger, A.F., Donner, R.M., Allen, H.D., Barst, R.J.: Collaborative care for adults with congenital heart disease. *Circulation* **105**(19), 2318–2323 (2002)
3. Liverani, A., Leali, F., Pellicciari, M.: Real-time 3D features reconstruction through monocular vision. *Int. J. Interact. Des. Manuf.* **4**(2), 103–112 (2010)
4. Furferi, R., Governi, L.: Machine vision tool for real-time detection of defects on textile raw fabrics. *J. Text. Inst.* **99**(1), 57–66 (2008)
5. Renzi, C., Leali, F., Cavazzuti, M., Andrisano, A.O.: A review on artificial intelligence applications to the optimal design of dedicated and reconfigurable manufacturing systems. *Int. J. Adv. Manuf. Technol.* **72**(1–4), 403–418 (2014)
6. Ploch, C.C., Mansi, C.S., Jayamohan, J., Kuhl, E.: Using 3D printing to create personalized brain models for neurosurgical training and preoperative planning. *World Neurosurg.* **90**, 668–674 (2016)
7. Burdall, O.C., Makin, E., Davenport, M., Ade-Ajayi, N.: 3D printing to simulate laparoscopic choledochal surgery. *J. Pediatr. Surg.* **51**(5), 828–831 (2016)
8. Wang, Y.T., Yang, X.J., Yan, B., Zeng, T.H., Qiu, Y.Y., Chen, S.J.: Clinical application of three-dimensional printing in the personalized treatment of complex spinal disorders. *Chin. J. Traumatol.* **19**(1), 31–34 (2016)
9. Giannopoulos, A.A., Mitsouras, D., Yoo, S.-J., Liu, P.P., Chatzizisis, Y.S., Rybicki, F.J.: Applications of 3D printing in cardiovascular diseases. *Nat. Rev. Cardiol.* **13**(12), 701–718 (2016)
10. Nocerino, E., Remondino, F., Ccheddu, F., Gallo, M., Gerosa, G.: 3D modelling and rapid prototyping for cardiovascular surgical planning—two case studies. *Int. Arch. Photogram. Remote Sens. Spat. Inf. Sci. ISPRS Arch.* **41**, 887–893 (2016)
11. Zhang, H., et al.: 4-D cardiac MR image analysis: left and right ventricular morphology and function. *IEEE Trans. Med. Imaging* **29**(2), 350–364 (2010)
12. Wu, J., Simon, M.A., Brigham, J.C.: A comparative analysis of global shape analysis methods for the assessment of the human right ventricle. *Comput. Methods Biomech. Biomed. Eng. Imaging Vis.* 1–17 (2014)
13. Punithakumar, Kumaradevan, et al.: Right ventricular segmentation in cardiac MRI with moving mesh correspondences. *Comput. Med. Imaging Graph.* **43**, 15–25 (2015)
14. Cappetti, N., Naddeo, A., Naddeo, F., Solitro, G.F.: Finite elements/Taguchi method based procedure for the identification of the geometrical parameters significantly affecting the biomechanical behavior of a lumbar disc. *Comput. Methods Biomech. Biomed. Eng.* (2015). doi:10.1080/10255842.2015.1128529
15. Huang, H.K.: Fundamentals of biomedical image processing. pp. 8–14 (1978)
16. Kahn Jr., C.E., Carrino, J.A., Flynn, M.J., Peck, D.J., Horii, S.C.: DICOM and radiology: past, present, and future. *J. Am. Coll. Radiol.* **4**(9), 652–657 (2007)
17. Rohrer, M., Bauer, H., Mintonovitch, J., Requardt, M., Weinmann, H.J.: Comparison of magnetic properties of MRI contrast media solutions at different magnetic field strengths. *Invest. Radiol.* **40**(11), 715–724 (2005)
18. Kuppusamy, P., Zweier, J.L.: A forward-subtraction procedure for removing hyperfine artifacts in electron paramagnetic resonance imaging. *Magn. Reson. Med.* **35**(3), 316–322 (1996)
19. Bersvendsen, J., Toews, M., Danudibroto, A., Wells, W.M., Urheim, S., Estépar, R.S.J., Samset, E.: Robust spatio-temporal registration of 4D cardiac ultrasound sequences. In: *Progress in Biomedical Optics and Imaging—Proceedings of SPIE*, 9790, art. no. 97900F (2016)
20. Renaud, J.M., Yip, K., Guimond, J., Trottier, M., Pibarot, P., Turcotte, E., Maguire, C., Lalonde, L., Gulenchyn, K., Farncombe, T.,

- 777 Wisenberg, G., Moody, J., Lee, B., Port, S.C., Turkington, T.G.,
778 Beanlands, R.S., Kemp, R.A.: Characterization of 3-dimensional
779 PET systems for accurate quantification of myocardial blood flow.
780 *J. Nucl. Med.* **58**(1), 103–109 (2017)
- 781 21. Stradiotti, P., Curti, A., Castellazzi, G., Zerbi, A.: Metal-related
782 artifacts in instrumented spine. Techniques for reducing artifacts
783 in CT and MRI: state of the art. *Eur. Spine J.* **18**(SUPPL. 1),
784 S102–S108 (2009)
- 785 22. Hill, D.L., Batchelor, P.G., Holden, M., Hawkes, D.J.: Medical
786 image registration. *Phys. Med. Biol.* **46**(3), R1 (2001)
- 787 23. Motwani, M.C., Gadiya, M.C., Motwani, R.C., Harris, F.C.: Sur-
788 vey of image denoising techniques. In: Proceedings of GSPX, pp.
789 27–30 (2004)
- 790 24. Draa, A., Benayad, Z., Djenna, F.Z.: An opposition-based firefly
791 algorithm for medical image contrast enhancement. *Int. J. Inf.*
792 *Commun. Technol.* **7**(4–5), 385–405 (2015)
- 793 25. Maini, R., Himanshu, A.: A comprehensive review of image
794 enhancement techniques. (2010). [arXiv:1003.4053](https://arxiv.org/abs/1003.4053)
- 795 26. Belaroussi, B., Milles, J., Carne, S., Zhu, Y.M., Benoit-Cattin,
796 H.: Intensity non-uniformity correction in MRI: existing methods
797 and their validation. *Med. Image Anal.* **10**(2), 234–246 (2006)
- 798 27. Vovk, U., Pernus, F., Likar, B.: A review of methods for correction
799 of intensity inhomogeneity in MRI. *IEEE Trans. Med. Imaging*
800 **26**(3), 405–421 (2007)
- 801 28. Ashburner, Friston: K.J.: Unified segmentation. *NeuroImage*
802 **26**(3), 839–851 (2005)
- 803 29. Johnston, B., Atkins, M.S., Mackiewicz, B., Anderson, M.: Seg-
804 mentation of multiple sclerosis lesions in intensity corrected
805 multispectral MRI. *IEEE Trans. Med. Imaging* **15**(2), 154–169
806 (1996)
- 807 30. Axel, L., Costantini, J., Listerud, J.: Intensity correction in
808 surface-coil MR imaging. *Am. J. Roentgenol.* **148**(2), 418–420
809 (1987)
- 810 31. Hou, Z.: A review on MR image intensity inhomogeneity correc-
811 tion. *Int. J. Biomed. Imaging* (2006)
- 812 32. Edelstein, W.A., Bottomley, P.A., Pfeifer, L.M.: A signal-to-noise
813 calibration procedure for NMR imaging systems. *Med. Phys.*
814 **11**(2), 180–185 (1984)
- 815 33. Rice, S.O.: Mathematical analysis of random noise. *Bell Syst.*
816 *Tech. J.* **23**, 282 (1944). (Reprinted by N. Wax, Selected Papers
817 on Noise and Stochastic Process, Dover Publication, 1954,
818 QA273W3)
- 819 34. Gudbjartsson, H., Patz, S.: The Rician distribution of noisy MRI
820 data. *Magnetic resonance in medicine? Soc. Magn. Reson. Med.*
821 **34**(6), 910–914 (1995)
- 822 35. Zhang, G., Yan, P., Zhao, H., Zhang, X.A.: contrast enhance-
823 ment algorithm for low-dose CT images based on local histogram
824 equalization. In: 2nd International Conference on Bioinformatics
825 and Biomedical Engineering, ICBBE 2008, art. no. 4535828, pp.
826 2462–2465 (2008)
- 827 36. Tan, T.L., Sim, K.S., Tso, C.P., Chong, A.K.: Contrast enhance-
828 ment of computed tomography images by adaptive histogram
829 equalization-application for improved ischemic stroke detection.
830 *Int. J. Imaging Syst. Technol.* **22**(3), 153–160 (2012)
- 831 37. Kim, Y.T.: Contrast enhancement using brightness preserving bi-
832 histogram equalization. *IEEE Trans. Consum. Electron.* **43**, 1–8
833 (1997)
- 834 38. Martorelli, M.: A new approach in CT artifact removal: three cases
835 study in maxillofacial surgery. *Int. J. Interact. Des. Manuf.* **7**(2),
836 115–124 (2013)
- 837 39. Ortiz, S.H., Contreras, T.: Chiu, Fox, M.D.: Ultrasound image
838 enhancement: a review. *Biomed. Signal Process. Control* **7**(5),
839 419–428 (2012)
- 840 40. Chen, Y., Yin, R., Flynn, P., Broschat, S.: Aggressive region grow-
841 ing for speckle reduction in ultra-sound images. *Pattern Recognit.*
842 *Lett.* **24**(4–5), 677–691 (2003)
41. Krissian, K., Westin, C.F., Kikinis, R., Vosburgh, K.G.: Oriented
843 speckle reducing anisotropic diffusion. *IEEE Trans. Image Pro-*
844 *cess.* **16**(5), 1412–1424 (2007)
- 845 42. Yong, Y., Croitoru, M.M., Bidani, A., Zwischenberger, J.B., Clark,
846 J.J.W.: Nonlinear multiscale wavelet diffusion for speckle sup-
847 pression and edge enhancement in ultrasound images. *IEEE Trans.*
848 *Med. Imaging* **25**(3), 297–311 (2006)
- 849 43. Finn, S., Glavin, M., Jones, E.: Echocardiographic speckle reduc-
850 tion comparison. *IEEE Trans. Ultrason. Ferroelectr. Freq. Control*
851 **58**(1), 82–101 (2011)
- 852 44. Michailovich, O.V., Adam, D.: A novel approach to the 2-d blind
853 deconvolution problem in medical ultrasound. *IEEE Trans. Med.*
854 *Imaging* **24**(1), 86–104 (2005)
- 855 45. Goerres, G.W., Hany, T.F., Kamel, E., et al.: Head and neck imag-
856 ing with PET and PET/CT: artefacts from dental metallic implants.
857 *Eur. J. Nucl. Med. Mol. Imaging* **29**(3), 367–70 (2002)
- 858 46. Lonn, A.H.R.: Evaluation of method to minimize the effect of
859 X-ray contrast in PETCT attenuation correction. In: 2003 IEEE
860 Nuclear Science Symposium, pp. 2220–2221 (2004)
- 861 47. Picard, Yani, Thompson, Christopher J.: Motion correction of
862 PET images using multiple acquisition frames. *IEEE Trans. Med.*
863 *Imaging* **16**(2), 137–144 (1997)
- 864 48. Pal, N.R., Pal, S.H.: A review on image segmentation techniques.
865 *Pattern Recognit.* **26**, 1277–1294 (1993)
- 866 49. Sharma, N., Aggarwal, L.M.: Automated medical image segmen-
867 tation techniques. *J. Med. Phys.* **35**(1), 3–14 (2010). doi:[10.4103/](https://doi.org/10.4103/0971-6203.58777)
868 [0971-6203.58777](https://doi.org/10.4103/0971-6203.58777)
- 869 50. McGuinness, K., O'Connor, N.: Toward automated evaluation
870 of interactive segmentation. *Comput. Vis. Image Understand.*
871 **115**(6), 868–884 (2011)
- 872 51. Kalshetti, P., Bunde, M., Rahangdale, P., Jangra, D., Chat-
873 topadhyay, C., Harit, G., Elhence, A.: An interactive medical
874 image segmentation framework using iterative refinement. *Com-*
875 *put. Biol. Med.* **83**, 22–33 (2017)
- 876 52. Hassan, K., Dort, J.C., Sutherland, G.R., Chan, S.: Evaluation
877 of software tools for segmentation of temporal bone anatomy.
878 Medicine meets virtual reality 22: NextMed/MMVR22, 220, 130.
879 In: Boykov, Y., Jolly, M.-P. (eds.) *Interactive Graph Cuts for Optimal*
880 *Boundary & Region Segmentation of Objects in n-d Images.*
881 *ICCV*, 2001, vol. 1, pp. 105–112 (2016)
- 882 53. Thomas, H.M.T., Devakumar, D., Sasidharan, B., Bowen, S.R.,
883 Heck, D.K., Samuel, E.J.J.: Hybrid positron emission tomogra-
884 phy segmentation of heterogeneous lung tumors using 3D Slicer:
885 improved GrowCut algorithm with threshold initialization. *J.*
886 *Med. Imaging* **4**(1), 011009–011009 (2017)
- 887 54. Zhao, Y., Zhu, S.C., Luo, S.: Co3 for ultra-fast and accurate
888 interactive segmentation. In: Proceedings of the International
889 Conference on Multimedia, pp. 93–102 (2010)
- 890 55. Peng, B., Zhang, L., Zhang, D.: A survey of graph theoretic
891 approaches to image segmentation. *Pattern Recognit.* **46**(3),
892 1020–1038 (2013)
- 893 56. Ecabert, O., et al.: Segmentation of the heart and great vessels
894 in CT images using a model-based adaptation framework. *Med.*
895 *Image Anal.* **15**(6), 863–876 (2011)
- 896 57. Schneider, R.J., Perrin, D.P., Vasilyev, N.V., Marx, G.R., Del Nido,
897 P.J., Howe, R.D.: Mitral annulus segmentation from 3D ultrasound
898 using graph cuts. *IEEE Trans. Med. Imaging* **29**(9), 1676–1687
899 (2010)
- 900 58. Zheng, Y., Barbu, A., Georgescu, B., Scheuering, M., Comaniciu,
901 D.: Four-chamber heart modeling and automatic segmentation
902 for 3-D cardiac CT volumes using marginal space learning and
903 steerable features. *IEEE Trans. Med. Imaging* **27**(11), 1668–1681
904 (2008)
- 905 59. Jolly, M.P.: Automatic segmentation of the left ventricle in cardiac
906 MR and CT images. *Int. J. Comput. Vis.* **70**(2), 151–163 (2006)
- 907

60. Ecabert, O., Peters, J., Weese, J.: Modeling shape variability for full heart segmentation in cardiac computed-tomography images. In: Medical Imaging International Society for Optics and Photonics, pp. 61443R–61443R (2006)
61. Kirişli, H.A., Gupta, V., Kirschbaum, S.W., Rossi, A., Metz, C.T., Schaap, M., van Geuns, R.J., Mollet, N., Lelieveldt, B.P., Reiber, J.H., van Walsum, T.: Comprehensive visualization of multimodal cardiac imaging data for assessment of coronary artery disease: first clinical results of the SMARTVis tool. *Int. J. Comput. Assist. Radiol. Surg.* **7**(4), 557–571 (2012)
62. Işgum, I., Staring, M., Rutten, A., Prokop, M., Viergever, V.A., Van Ginneken, B.: Multi-atlas-based segmentation with local decision fusion—application to cardiac and aortic segmentation in CT scans. *IEEE Trans. Med. Imaging* **28**(7), 1000–1010 (2009)
63. Dey, D., Suzuki, Y., Suzuki, S., Ohba, M., Slomka, P.J., Polk, D., Shaw, L.J., Berman, D.S.: Automated quantitation of pericardiac fat from noncontrast CT. *Invest. Radiol.* **43**(2), 145–153 (2008)
64. Mühlenbruch, G., Das, M., Hohl, C., Wildberger, J.E., Rinck, D., Flohr, T.G., Koos, R., Knackstedt, C., Günther, R.W., Mahnken, A.H.: Global left ventricular function in cardiac CT. Evaluation of an automated 3D region-growing segmentation algorithm. *Eur. Radiol.* **16**(5), 1117–1123 (2006)
65. Juergens, K.U., Seifarth, H., Range, F., Wienbeck, S., Wenker, M., Heindel, W., Fischbach, R.: Automated threshold-based 3D segmentation versus short-axis planimetry for assessment of global left ventricular function with dual-source MDCT. *Am. J. Roentgenol.* **190**(2), 308–314 (2008)
66. Yalamanchili, R., Dey, D., Kukure, U., Nakazato, R., Berman, D.S., Kakadiaris, I.A.: Knowledge-based quantification of pericardial fat in non-contrast CT data. In: SPIE Medical Imaging International Society for Optics and Photonics, pp. 76231X–76231X (2010)
67. Margeta, J., McLeod, K., Criminisi, A., Ayache, N.: Decision forests for segmentation of the left atrium from 3D MRI. In: International Workshop on Statistical Atlases and Computational Models of the Heart, pp. 49–56 (2013)
68. Lopez-Perez, A., Sebastian, R., Ferrero, J.M.: Three-dimensional cardiac computational modelling: methods, features and applications. *BioMed. Eng. Online* **14**(1) (2015)
69. Trunk, P., Mocnik, J., Trobec, R., Gersak, B.: 3D heart model for computer simulations in cardiac surgery. *Comput. Biol. Med.* **37**, 1398–1403 (2007)
70. Ecabert, O., Peters, J., Schramm, H., Lorenz, C., von Berg, J., Walker, M.J., et al.: Automatic model-based segmentation of the heart in CT images. *IEEE Trans. Med. Imaging* **27**, 1189–1201 (2008)
71. Ivanc, T., Lorenz, C., von Berg, J., et al.: Segmentation of the heart and great vessels in CT images using a model-based adaptation framework. *Med. Image Anal.* **15**, 863–76 (2011)
72. Schulte, R.F., Sands, G.B., Sachse, F.B., Dössel, O., Pullan, A.J.: Creation of a human heart model and its customisation using ultrasound images. *Biomed. Tech. Eng.* **46**, 26–28 (2001)
73. Wenk, J.F., Zhang, Z., Cheng, G., Malhotra, D., Acevedo-Bolton, G., Burger, M., et al.: First finite element model of the left ventricle with mitral valve: insights into ischemic mitral regurgitation. *Ann. Thorac. Surg.* **89**, 1546–53 (2010)
74. Ruiz-Villa, C.A., Tobón, C., Rodríguez, J.F., Ferrero, J.M., Hornero, F., Saíz, J.: Influence of atrial dilatation in the generation of re-entries caused by ectopic activity in the left atrium. *Comput. Cardiol.* **36**, 457–460 (2009)
75. Seemann, G., Höper, C., Sachse, F.B., Dössel, O., Holden, A.V., Zhang, H.: Heterogeneous three-dimensional anatomical and electrophysiological model of human atria. *Philos. Trans. R. Soc. A Math. Phys. Eng. Sci.* **364**, 1465–1481 (2006)
76. Zhao, J., Butters, T.D., Zhang, H., LeGrice, I.J., Sands, G.B., Smaill, B.H.: Image-based model of atrial anatomy and electrical activation: a computational platform for investigating atrial arrhythmia. *IEEE Trans. Med. Imaging* **32**, 18–27 (2013)
77. Bishop, M.J., Plank, G., Burton, R.A.B., Schneider, J.E., Gavigan, D.J., Grau, V., et al.: Development of an anatomically detailed MRI-derived rabbit ventricular model and assessment of its impact on simulations of electrophysiological function. *Am. J. Physiol. Heart Circ. Physiol.* **298**, H699–718 (2010)
78. Lorensen, W.E., Cline, H.E.: Marching cubes: a high resolution 3D surface construction algorithm. In: *ACM Siggraph Computer Graphics*, vol. 21(4), pp. 163–169. ACM (1987)
79. Han, C.Y., Porembka, D.T., Lin, K.-N.: Method for automatic contour extraction of a cardiac image. U.S. Patent No. 5,457,754. 10 (1995)
80. Di Angelo, L., Di Stefano, P., Giaccari, L.: A new mesh-growing algorithm for fast surface reconstruction. *Comput. Aid. Des.* **43**(6), 639–650 (2011)
81. Angelo, L.Di, Stefano, P.Di, Giaccari, L.: A fast mesh-growing algorithm for manifold surface reconstruction. *Comput. Aid. Des. Appl.* **10**(2), 197–220 (2013)
82. Young, P.G., Beresford-West, T.B.H., Coward, S.R.L., Notarberardino, B., Walker, B., Abdul-Aziz, A.: An efficient approach to converting three-dimensional image data into highly accurate computational models. *Philos. Trans. R. Soc. Lond. A Math. Phys. Eng. Sci.* **366**(1878), 3155–3173 (2008)
83. Simões, B., Riggio, M., de Amicis, R.: Modeling morphological features of timber from X-ray tomographic images. *Int. J. Interact. Des. Manuf.* **6**(2), 65–73 (2012)
84. Muscia, R.: Hybrid modelization of intracoronary stents. *Int. J. Interact. Des. Manuf.* **8**(4), 305–315 (2014)
85. Furferi, R., Governi, L., Palai, M., Volpe, Y.: From unordered point cloud to weighted B-spline—a novel PCA-based method. In: *Applications of Mathematics and Computer Engineering—American Conference on Applied Mathematics, AMERICAN-MATH'11, 5th WSEAS International Conference on Computer Engineering and Applications, CEA'11*, pp. 146–151 (2011)
86. Governi, L., Furferi, R., Puggelli, L., Volpe, Y.: Improving surface reconstruction in shape from shading using easy-to-set boundary conditions. *Int. J. Comput. Vis. Robot.* **3**(3), 225–247 (2013)
87. Furferi, R., Governi, L., Palai, M., Volpe, Y.: Multiple incident splines (MISs) algorithm for topological reconstruction of 2D unordered point clouds. *Int. J. Math. Comput. Simul.* **5**(2), 171–179 (2011)
88. Volpe, Y., Furferi, R., Governi, L., Tennirelli, G.: Computer-based methodologies for semi-automatic 3D model generation from paintings. *Int. J. Comput. Aid. Eng. Technol.* **6**(1), 88–112 (2014)
89. Colli Franzone, P., Guerri, L., Pennacchio, M., Taccardi, B.: Spread of excitation in 3-D models of the anisotropic cardiac tissue. II. Effects of fiber architecture and ventricular geometry. *Math. Biosci.* **147**, 131–71 (1998)
90. Kerckhoffs, R.C.P., Bovendeerd, P.H.M., Kotte, J.C.S., Prinzen, F.W., Smits, K., Arts, T.: Homogeneity of cardiac contraction despite physiological asynchrony of depolarization: a model study. *Ann. Biomed. Eng.* **31**, 536–47 (2003)
91. Romero, D., Sebastian, R., Bijnens, B.H., Zimmerman, V., Boyle, P.M., Vigmond, E.J., et al.: Effects of the purkinje system and cardiac geometry on biventricular pacing: a model study. *Ann. Biomed. Eng.* **38**, 1388–1398 (2010)
92. Ordas, S., Oubel, E., Sebastian, R., Frangi, A.F.: Computational anatomy atlas of the heart. In: *5th International Symposium on Image Signal Processing and Analysis (ISPA 2007)*. Istanbul, Turkey. IEEE, pp. 338–342 (2007)
93. Streeter Jr., D.D., Spotnitz, H.M., Patel, D.P., Ross Jr., J., Sonnenblick, E.H.: Fiber orientation in the canine left ventricle during diastole and systole. *Circ. Res.* **24**, 339–347 (1969)

- 1040 94. Vandenbroucke, B., Kruth, J.P.: Selective laser melting of biocompatible metals for rapid manufacturing of medical parts. *Rapid Prototyp. J.* **13**(4), 196–203 (2007) 1061
- 1041 95. Markwald, R.R.: Organ printing: computer-aided jet-based 3D 1062
- 1042 tissue engineering. *Trends Biotechnol.* **21**(4), 157–161 (2003) 1063
- 1043 96. XXXX 1064
- 1044 97. XXXX 1065
- 1045 98. Miner, S., Nield, L.: Left atrial appendage closure guided by 1066
- 1046 personalized 3D-printed cardiac reconstruction. *Lett. Editor* **8**(7) 1067
- 1047 (2015) 1068
- 1048 99. Liu, P., Liu, R., Zhang, Y., Liu, Y., Tang, X., Cheng, Y.: The 1069
- 1049 value of 3D printing models of left atrial appendage using real- 1070
- 1050 time 3D transesophageal echocardiographic data in left atrial 1071
- 1051 appendage occlusion: applications toward an era of truly personal- 1072
- 1052 ized medicine. *Cardiology* **135**(4), 255–261 (2016) 1073
- 1053 100. Pepper, J., Petrou, M., Rega, F., Rosendahl, U., Golesworthy, 1074
- 1054 T., Treasure, T.: Implantation of an individually computer- 1075
- 1055 designed and manufactured external support for the Marfan 1076
- 1056 aortic root. In: *Multimedia Manual of Cardiothoracic Surgery: 1077*
- 1057 MMCTS/European Association for Cardio-Thoracic Surgery, p. 1078
- 1058 mmt004 (2013) 1079
- 1059 101. Tam, M.D., Latham, T., Brown, J.R.I., Jakeways, M.: Use of a 3D 1061
- 1060 printed hollow aortic model to assist EVAR planning in a case 1062
- 1061 with complex neck anatomy: Potential of 3D printing to improve 1063
- 1062 patient outcome. *J. Endovasc. Ther.* **21**(5), 760–764 (2014) 1064
- 1063 102. Chaowu, Y., Hua, L., Xin, S.: Three-dimensional printing as an 1065
- 1064 aid in transcatheter closure of secundum atrial septal defect with 1066
- 1065 rim deficiency: in vitro trial occlusion based on a personalized 1067
- 1066 heart model. *Circulation* **133**(17), e608–e610 (2016) 1068
- 1067 103. Yang, D.H., Kang, J.-W., Kim, N., Song, J.-K., Lee, J.-W., Lim, 1069
- 1068 T.-H.: Myocardial 3-dimensional printing for septal myectomy 1070
- 1069 guidance in a patient with obstructive hypertrophic cardiomyopa- 1071
- 1070 thy. *Circulation* **132**(4), 300–301 (2015) 1072
- 1071 104. Giannopoulos, A.A., Steigner, M.L., George, E., Barile, M., 1073
- 1072 Hunsaker, A.R., Rybicki, F.J., Mitsouras, D.: Cardiothoracic 1074
- 1073 applications of 3-dimensional printing. *J. Thorac. Imaging* **31**(5), 1075
- 1074 253–272 (2016) 1076
- 1075 105. Marsden, A.L., Feinstein, J.A.: Computational modeling and 1077
- 1076 engineering in pediatric and congenital heart disease. *Curr. Opin. 1078*
- 1077 *Pediatr.* **27**(5), 587 (2015) 1079

Author Query Form

**Please ensure you fill out your response to the queries raised below
and return this form along with your corrections**

Dear Author

During the process of typesetting your article, the following queries have arisen. Please check your typeset proof carefully against the queries listed below and mark the necessary changes either directly on the proof/online grid or in the 'Author's response' area provided below

Query	Details required	Author's response
1.	Please check and confirm the inserted organisation name is correct for the Affiliation 1 and amend if necessary.	
2.	Please check and confirm if the inserted citation of Fig. 6 is correct. If not, please suggest an alternate citation. Please note that figures should be cited sequentially in the text.	
3.	References [96, 97] are cited in the text, but not provided in the list. Please provide the references in the list or delete these citations.	
4.	Please provide volume number for the reference [12].	
5.	Please provide complete details for the references [15, 78].	
6.	Please provide volume number and page range for the reference [31].	
7.	Please check and confirm the inserted initial is correct for the author "Zhao" in reference [54].	
8.	Please provide page range for the references [68, 98].	